



## On-chip two-mode division multiplexing using tapered directional coupler-based mode multiplexer and demultiplexer

Ding, Yunhong; Xu, Jing; Da Ros, Francesco; Huang, Bo; Ou, Haiyan; Peucheret, Christophe

*Published in:*  
Optics Express

*Link to article, DOI:*  
[10.1364/OE.21.010376](https://doi.org/10.1364/OE.21.010376)

*Publication date:*  
2013

*Document Version*  
Publisher's PDF, also known as Version of record

[Link back to DTU Orbit](#)

*Citation (APA):*  
Ding, Y., Xu, J., Da Ros, F., Huang, B., Ou, H., & Peucheret, C. (2013). On-chip two-mode division multiplexing using tapered directional coupler-based mode multiplexer and demultiplexer. *Optics Express*, 21(8), 10376-10382. <https://doi.org/10.1364/OE.21.010376>

---

### General rights

Copyright and moral rights for the publications made accessible in the public portal are retained by the authors and/or other copyright owners and it is a condition of accessing publications that users recognise and abide by the legal requirements associated with these rights.

- Users may download and print one copy of any publication from the public portal for the purpose of private study or research.
- You may not further distribute the material or use it for any profit-making activity or commercial gain
- You may freely distribute the URL identifying the publication in the public portal

If you believe that this document breaches copyright please contact us providing details, and we will remove access to the work immediately and investigate your claim.

# On-chip two-mode division multiplexing using tapered directional coupler-based mode multiplexer and demultiplexer

Yunhong Ding,<sup>1,\*</sup> Jing Xu,<sup>1</sup> Francesco Da Ros,<sup>1</sup> Bo Huang,<sup>1,2</sup> Haiyan Ou,<sup>1</sup> and Christophe Peucheret<sup>1</sup>

<sup>1</sup>Department of Photonics Engineering, Technical University of Denmark, 2800 Kgs. Lyngby, Denmark

<sup>2</sup>Wuhan National Laboratory for Optoelectronics, School of Optoelectronics Science and Engineering, Huazhong University of Science and Technology, Wuhan, 430074, Hubei, China

\*yudin@fotonik.dtu.dk

**Abstract:** We demonstrate a novel on-chip two-mode division multiplexing circuit using a tapered directional coupler-based TE<sub>0</sub>&TE<sub>1</sub> mode multiplexer and demultiplexer on the silicon-on-insulator platform. A low insertion loss (0.3 dB), low mode crosstalk (< -16 dB), wide bandwidth (~100 nm), and large fabrication tolerance (20 nm) are measured. An on-chip mode multiplexing experiment is carried out on the fabricated circuit with non return-to-zero (NRZ) on-off keying (OOK) signals at 40 Gbit/s. The experimental results show clear eye diagrams and moderate power penalty for both TE<sub>0</sub> and TE<sub>1</sub> modes.

©2013 Optical Society of America

**OCIS codes:** (130.3120) Integrated optics devices; (030.4070) Modes; (060.4230) Multiplexing; (200.4650) Optical interconnects.

---

## References and links

1. R. Kirchain and L. Kimerling, "A roadmap for nanophotonics," *Nat. Photonics* **1**(6), 303–305 (2007).
2. B. G. Lee, X. Chen, A. Biberman, X. Liu, I. W. Hsieh, C. Y. Chou, J. I. Dadap, F. Xia, W. M. J. Green, L. Sekaric, Y. A. Vlasov, R. M. Osgood, and K. Bergman, "Ultrahigh-bandwidth silicon photonic nanowire waveguides for on-chip networks," *IEEE Photon. Technol. Lett.* **20**(6), 398–400 (2008).
3. S. Berdagué and P. Facq, "Mode division multiplexing in optical fibers," *Appl. Opt.* **21**(11), 1950–1955 (1982).
4. G. J. Veldhuis, J. H. Berends, and P. V. Lambeck, "Design and characterization of a mode-splitting  $\Psi$ -junction," *J. Lightwave Technol.* **14**(7), 1746–1752 (1996).
5. K. Shirafuji and S. Kurazono, "Transmission characteristics of optical asymmetric Y junction with a gap region," *J. Lightwave Technol.* **9**(4), 426–429 (1991).
6. J. D. Love and N. Riesen, "Single-, few-, and multimode Y-junctions," *J. Lightwave Technol.* **30**(3), 304–309 (2012).
7. N. Riesen and J. D. Love, "Design of mode-sorting asymmetric Y-junctions," *Appl. Opt.* **51**(15), 2778–2783 (2012).
8. Y. Kawaguchi and K. Tsutsumi, "Mode multiplexing and demultiplexing devices using multimode interference couplers," *Electron. Lett.* **38**(25), 1701–1702 (2002).
9. T. Uematsu, Y. Ishizaka, Y. Kawaguchi, K. Saitoh, and M. Koshiba, "Design of a compact two-mode multi/demultiplexer consisting of multimode interference waveguides and a wavelength-insensitive phase shifter for mode-division multiplexing transmission," *J. Lightwave Technol.* **30**(15), 2421–2426 (2012).
10. M. Greenberg and M. Orenstein, "Multimode add-drop multiplexing by adiabatic linearly tapered coupling," *Opt. Express* **13**(23), 9381–9387 (2005).
11. M. Greenberg and M. Orenstein, "Simultaneous dual mode add/drop multiplexers for optical interconnects buses," *Opt. Commun.* **266**(2), 527–531 (2006).
12. S. Bagheri and W. M. J. Green, "Silicon-on-insulator mode-selective add-drop unit for on-chip mode-division multiplexing," in *Proceedings of IEEE Group IV Photonics Conference* (San Francisco, United States of America, 2009), 166–168.
13. D. Dai, "Silicon mode-(de)multiplexer for a hybrid multiplexing system to achieve ultrahigh capacity photonic networks-on-chip with a single-wavelength-carrier light," in *Asia Communications and Photonics Conference*, (Guangzhou, China, 2012), AT3B.3.
14. N. Hanzawa, K. Saitoh, T. Sakamoto, T. Matsui, S. Tomita, and M. Koshiba, "Asymmetric parallel waveguide with mode conversion for mode and wavelength division multiplexing transmission," in *Optical Fiber Communication Conference*, OSA Technical Digest (Optical Society of America, 2012), paper OTu11.4.

## 1. Introduction

On-chip optical interconnections based on silicon-on-insulator (SOI) nanowires are a promising technology for future massively-parallel chip multiprocessors [1]. Compared to traditional copper wire-based electrical interconnects, silicon-based on-chip optical interconnects offer broad bandwidth, allowing to reach very high capacities using the wavelength-division multiplexing (WDM) technology [2]. Mode-division multiplexing (MDM) offers a new dimension to increase the capacity of SOI optical links [3]. The key to realize on-chip MDM is an efficient mode (de)multiplexer. On-chip mode multiplexers based on weakly guiding asymmetrical  $\Psi$ - and Y- junctions have been suggested [4–7]. Multimode interferometers have also been proposed as mode multiplexers [8, 9]. Recently, mode multiplexers based on asymmetrical directional couplers (DCs) have also been proposed [10–14]. However, those structures are limited by their sensitivity to fabrication errors. Currently, an efficient mode multiplexer built on the SOI platform with low insertion loss, low crosstalk, and large fabrication tolerance is still unreported.

A tapered DC has been shown to be an efficient design in order to relax the fabrication tolerance of conventional asymmetrical normal DCs used as polarization splitters and rotators [15]. In this paper we demonstrate an on-chip two-mode division multiplexing circuit using a tapered DC-based  $TE_0$ & $TE_1$  multiplexer and demultiplexer. The device can furthermore be fabricated by a simple process on the SOI platform. A minimum insertion loss of 0.3 dB and mode crosstalk lower than  $-16$  dB over a wide bandwidth of 100 nm are demonstrated together with a large tolerance of more than 20 nm for the width deviation of the narrow silicon waveguide (compared to only a few nanometers for a normal DC) and with relaxed coupling length sensitivity. The chip is further employed in a system experiment where two non return-to-zero (NRZ) on-off keying (OOK) channels, each modulated at 40 Gbit/s, are mode-multiplexed and demultiplexed. The experimental results show clear eye-diagrams, and only 1.6 dB and 1.8 dB power penalty for the two demultiplexed channels. To the best of our knowledge, this is the first system demonstration of on-chip mode multiplexing on an SOI waveguide for interconnect applications.

## 2. Principle and design of the $TE_0$ & $TE_1$ mode multiplexer

The  $TE_0$ & $TE_1$  mode multiplexer is based on a tapered DC, which parallel-couples a narrow silicon waveguide (waveguide width  $w_1$ ) to a wide tapered waveguide (from  $w_{2a}$  to  $w_{2b}$  with center width of  $w_2$ ) with a coupling length and gap of  $L$  and  $g$ , respectively, as shown in Fig. 1. The structure is degenerated to a conventional asymmetrical normal DC when  $w_{2a} = w_{2b} = w_2$ . For conventional DC-based  $TE_0$ & $TE_1$  mode multiplexers, the  $TE_0$ - $TE_1$  coupling relies on the phase matching between the waveguides, i.e. the effective refractive index of the  $TE_0$  mode of the narrow waveguide should be equal to that of the  $TE_1$  mode of the wide waveguide. In this case, if  $TE_0$  light is injected into the narrow waveguide, a high coupling efficiency  $r_{TE_0-TE_1}$  will be obtained at the output of the wide waveguide. On the other hand, because of the significant effective refractive index difference between the  $TE_0$  modes in the two asymmetrical waveguides, a very low coupling efficiency  $r_{TE_0-TE_0}$  (mode crosstalk) is obtained. However, in conventional asymmetrical DCs, the phase matching can be easily destroyed by fabrication errors of the narrow waveguide. A fabrication error-induced width deviation  $\Delta w$  will result in a larger effective refractive index deviation  $\Delta n_{eff}$  for the narrow waveguide than for the wide waveguide since the slope of the effective index of the  $TE_0$  mode

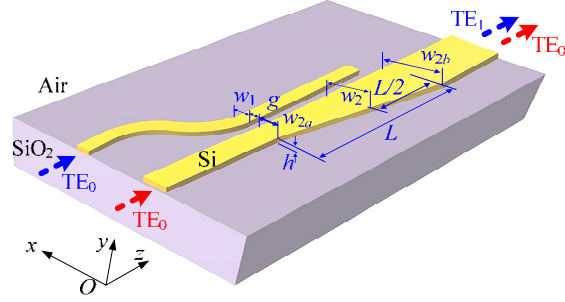


Fig. 1. Schematic structure of the proposed TE<sub>0</sub>&TE<sub>1</sub> multiplexer.

versus waveguide width is larger than that of the TE<sub>1</sub> mode, as shown in Fig. 2(a). The larger the slope difference, the easier it is for the phase matching condition to be destroyed due to waveguide width errors. Moreover, the length of the DC should be properly designed to avoid the converted TE<sub>1</sub> light coupling back to the narrow waveguide. In order to relax these limitations, the wide waveguide is tapered from  $w_{2a}$  to  $w_{2b}$  in our proposed design. For the two widths  $w_{2a}$  and  $w_{2b}$  of the wide waveguide, the corresponding widths of the narrow waveguide enabling to satisfy the phase matching condition are  $w_{1a}$  and  $w_{1b}$ , respectively, as indicated in Fig. 2(a). Consequently, tapering the wide waveguide from  $w_{2a}$  to  $w_{2b}$  will result in a deviation tolerance between  $w_{1a}$  and  $w_{1b}$  for the narrow waveguide because a phase matching position can always be found along the taper. After the phase matching position, the conversion efficiency will be maintained and the fabrication error sensitivity of the coupling length will be relaxed. It should be noted that  $w_{2a}$  should not be too close to the width where the TE<sub>1</sub> and TM<sub>0</sub> modes are hybridized (700 nm in our case). A large tapering strength (width difference between  $w_{2a}$  and  $w_{2b}$ ) provides a larger fabrication tolerance (from  $w_{1a}$  to  $w_{1b}$ ) for the narrow waveguide. However, a larger tapering strength requires a longer tapering length  $L$  in order to achieve a sufficiently long effective coupling length around the phase matching position. Widths  $w_1 = 390$  nm and  $w_2 = 800$  nm were chosen as a starting point since these widths satisfy the phase matching condition, as shown in Fig. 2(a). Tapering from  $w_{2a} = 750$  nm to  $w_{2b} = 850$  nm with center width  $w_2$  is selected for the wide waveguide. Figure 2(b) shows the TE<sub>0</sub>-TE<sub>1</sub> coupling efficiency  $r_{\text{TE0-TE1}}$  and mode crosstalk  $r_{\text{TE0-TE0}}$  simulated as a function of wavelength using the eigenmode expansion (EME) method [16] with  $L = 50$   $\mu\text{m}$  and  $g = 100$  nm. The residual TE<sub>0</sub>-TM<sub>0</sub> coupling  $r_{\text{TE0-TM0}}$  is also shown. One can find that a high  $r_{\text{TE0-TE1}}$  with  $r_{\text{TE0-TE0}}$  lower than  $-22$  dB are obtained over a large wavelength range of 200 nm. In addition, a very small  $r_{\text{TE0-TM0}}$  lower than  $-30$  dB is also obtained thanks to the large refractive index difference between these two modes.

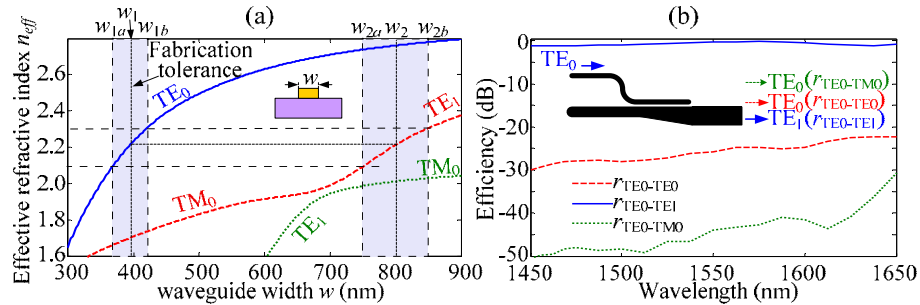


Fig. 2. (a) Effective indices of the TE<sub>0</sub>, TE<sub>1</sub> and TM<sub>0</sub> modes of an air-clad SOI waveguide as a function of the waveguide width  $w$  for a waveguide height  $h = 250$  nm. (b) Simulated TE<sub>0</sub>-TE<sub>1</sub> coupling efficiency  $r_{\text{TE0-TE1}}$ , mode crosstalk  $r_{\text{TE0-TE0}}$ , and TE<sub>0</sub>-TM<sub>0</sub> coupling efficiency  $r_{\text{TE0-TM0}}$  as a function of wavelength.  $w_1 = 390$  nm,  $w_{2a} = 750$  nm,  $w_{2b} = 850$  nm,  $L = 50$   $\mu\text{m}$  and  $g = 100$  nm.

As mentioned previously, since the coupling efficiency  $r_{\text{TE}_0\text{-TE}_1}$  is much more sensitive to the width of the narrow waveguide than to that of the wide waveguide, only the sensitivity to the width deviation of the narrow waveguide is investigated. The width of the narrow waveguide is changed between  $w_1 \pm \Delta w$  to investigate the fabrication tolerance, where  $\Delta w$  is the width deviation due to fabrication error. A coupling gap  $g = 100$  nm is selected. Figures 3(a) and 3(b) show the calculated coupling efficiency  $r_{\text{TE}_0\text{-TE}_1}$  and mode crosstalk  $r_{\text{TE}_0\text{-TE}_0}$  as a function of the width deviation  $\Delta w$  and coupling gap  $g$ , respectively, for both tapered and normal DCs. One can find that  $r_{\text{TE}_0\text{-TE}_0}$  shows good tolerance to the width deviation  $\Delta w$  for both tapered and normal DCs since the phase mismatch of  $\text{TE}_0\text{-TE}_0$  coupling is large in both cases. In case of a tapered DC, a high  $r_{\text{TE}_0\text{-TE}_1}$  with  $r_{\text{TE}_0\text{-TE}_0}$  lower than  $-25$  dB is obtained within a width deviation range of about 40 nm for  $L$  varying from 30  $\mu\text{m}$  to 50  $\mu\text{m}$ . Since a high  $r_{\text{TE}_0\text{-TE}_1}$  is maintained as  $L$  further increases, the width deviation tolerance is also expected for  $L$  longer than 50  $\mu\text{m}$ . In addition, the tapered DC-based scheme also exhibits a good tolerance to the coupling gap, and a better gap tolerance is obtained for longer  $L$ . However, in the case of a normal DC, the width deviation tolerance is only a few nanometers, and the gap tolerance is even worse than for a tapered DC. Moreover,  $r_{\text{TE}_0\text{-TE}_1}$ , the width deviation tolerance, and the gap tolerance are much more sensitive to  $L$  than in the case of tapered DC.

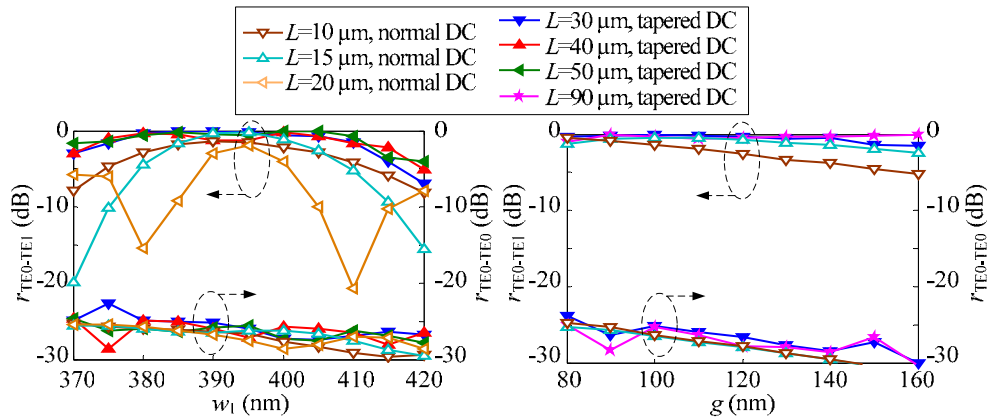


Fig. 3. Simulated coupling efficiency  $r_{\text{TE}_0\text{-TE}_1}$  and mode crosstalk  $r_{\text{TE}_0\text{-TE}_0}$  as a function of (a) width deviation  $\Delta w$  and (b) coupling gap  $g$  for different lengths  $L$  for both tapered and normal DCs. The operation wavelength is 1550 nm.

### 3. Device fabrication and characterization

Based on the proposed  $\text{TE}_0\text{&TE}_1$  mode multiplexer design, a two-mode division multiplexing circuit was fabricated on a SOI wafer with 250 nm top silicon layer and 3  $\mu\text{m}$  buried silicon dioxide by a single step of E-beam lithography (JEOL JBX-9500FS) and inductively coupled plasma reactive ion etching (STS Advanced Silicon Etcher). Polymer (SU8-2005) waveguides of dimensions  $3.5 \mu\text{m} \times 3.5 \mu\text{m}$  covering silicon inverse tapers were fabricated afterwards in order to reduce the coupling loss to tapered fibers. Figure 4(a) shows the fabricated device, which consists of a multiplexer (detailed in Fig. 4(b)) at the input side, a multimode data bus (750 nm wide), and a demultiplexer (identical to the multiplexer) at the output side. The width of the narrow waveguide is 355 nm, the wide waveguide is tapered from 748 nm to 848 nm, and the coupling gap is 100 nm, as shown in Figs. 4(c) and 4(d). Figure 5(a) shows the measured transmissions (normalized to a straight waveguide) from inputs  $\text{CH}_1$  and  $\text{CH}_2$  to the demultiplexed outputs  $\text{CH}_1$  and  $\text{CH}_2$ , respectively, on the  $\text{TE}_0$  mode, and the corresponding mode crosstalk (from inputs  $\text{CH}_1$  and  $\text{CH}_2$  to the demultiplexed outputs  $\text{CH}_2$  and  $\text{CH}_1$  on the  $\text{TE}_0$  mode, respectively) for different widths  $w_1$  of the narrow

waveguide and taper lengths  $L$ . High transmission from  $CH_1$  and  $CH_2$  to the corresponding demultiplexed  $CH_1$  and  $CH_2$  with lowest insertion loss of 0.3 dB and crosstalk lower than  $-16$  dB are obtained over a large bandwidth of 100 nm for narrow waveguide widths of 360 nm and 380 nm, and taper length of 30  $\mu\text{m}$  and 50  $\mu\text{m}$ .

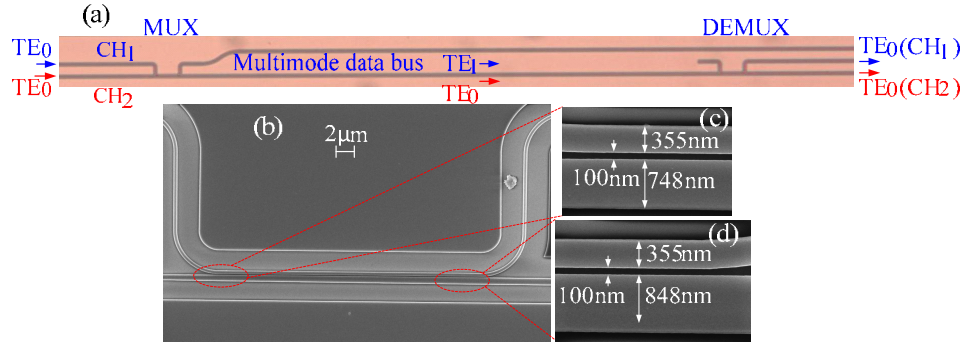


Fig. 4. (a) Fabricated  $TE_0$ & $TE_1$  mode multiplexing circuit. (b) Scanning electron microscope (SEM) pictures of a fabricated  $TE_0$ & $TE_1$  mode (de)multiplexer and details of its beginning (c) and end (d) sides.

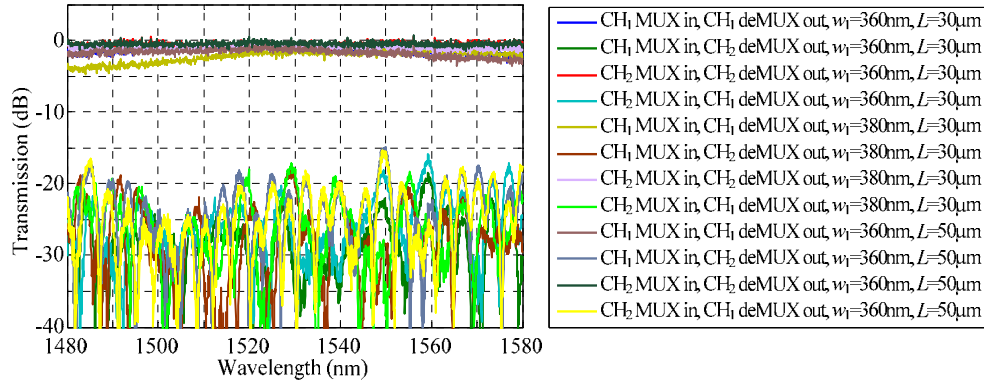


Fig. 5. Measured transmissions from inputs  $CH_1$  and  $CH_2$  to the demultiplexed outputs  $CH_1$  and  $CH_2$  on the  $TE_0$  mode, and the corresponding crosstalk for different widths  $w_1$  of the narrow waveguide and taper lengths  $L$ .

#### 4. System demonstration

The fabricated chip was further employed for two-mode division multiplexing application with NRZ-OOK signals at 40 Gbit/s. Figure 6 shows the experimental setup. Continuous wave (CW) light at 1553.06 nm is modulated at 40 Gbit/s in the NRZ-OOK format in a Mach-Zehnder modulator with a pseudo-random binary pattern length of  $2^{31}-1$ , and then amplified by an erbium-doped fiber amplifier (EDFA). The amplified signal is split into two tributaries by a 3 dB coupler afterward. Before being injected into the silicon chip, the two tributaries are decorrelated using a length of 1 km standard single mode fiber. Polarization controllers (PCs) are used in order to set the state of polarization of each tributary so that it excites the  $TE$  mode of the silicon chip. The two channels, labeled  $CH_1$  and  $CH_2$ , are then simultaneously injected into the chip using a lensed fiber array for on-chip two-mode division multiplexing. The demultiplexed output signals from the chip are finally detected in a preamplified receiver.

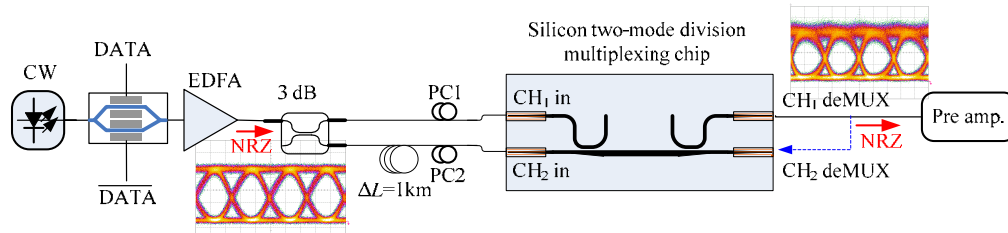


Fig. 6. Experimental setup for on-chip two-mode division multiplexing. The insets show the measured eye-diagrams of the NRZ signals after the transmitter and at one of the outputs of the demultiplexer, respectively.

Figure 7(a) shows the spectra of the signals recorded at the CH<sub>1</sub> and CH<sub>2</sub> demultiplexing ports when only either the CH<sub>1</sub> or CH<sub>2</sub> signal are injected into the waveguide, respectively. They correspond to either TE<sub>1</sub> mode or TE<sub>0</sub> mode propagation in the silicon multimode data bus, respectively. Crosstalk spectra (measured at CH<sub>2</sub> output with CH<sub>1</sub> excitation and at CH<sub>1</sub> output with CH<sub>2</sub> excitation) are also represented. Since the signal wavelength is tuned to the dip wavelength of the crosstalk spectrum (detailed in Fig. 5), a low crosstalk level below  $-20$  dB is obtained for both channels. The corresponding demultiplexed signals exhibit clear eye diagrams, as shown in Figs. 7(c) and 7(d) when only the TE<sub>1</sub> or the TE<sub>0</sub> mode is propagating in the waveguide. When both TE<sub>1</sub> and TE<sub>0</sub> modes are multiplexed, clear eye diagrams are also obtained for the two demultiplexed signals thanks to the low mode crosstalk, as shown in Figs. 7(e) and 7(f). Figure 8 shows the results of bit-error-ratio (BER) measurements performed for the signals from the CH<sub>1</sub> and CH<sub>2</sub> demultiplexing ports with and without crosstalk. Low power penalties of 1.6 dB and 1.8 dB are obtained for CH<sub>1</sub> and CH<sub>2</sub> demultiplexing with crosstalk, respectively.

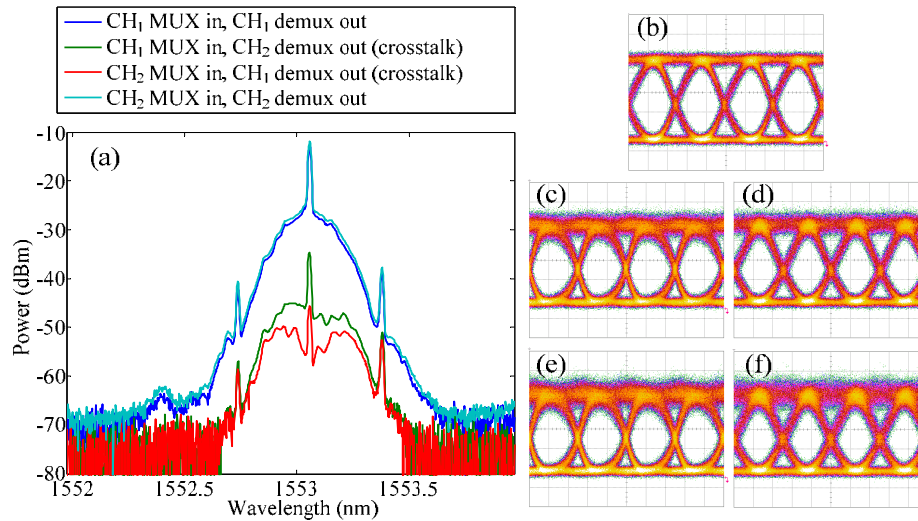


Fig. 7. (a) Measured spectra of the two demultiplexed NRZ-OOK signals at output ports CH<sub>1</sub> and CH<sub>2</sub>, as well as the corresponding crosstalk for each demultiplexing channel. (b) Measured eye diagrams of the NRZ-OOK signal at the transmitter output. Measured eye-diagrams of the demultiplexed signal at the CH<sub>1</sub> output port without (c) and with (e) crosstalk. Measured eye-diagrams of the demultiplexed signal at the CH<sub>2</sub> output port without (d) and with (f) crosstalk.



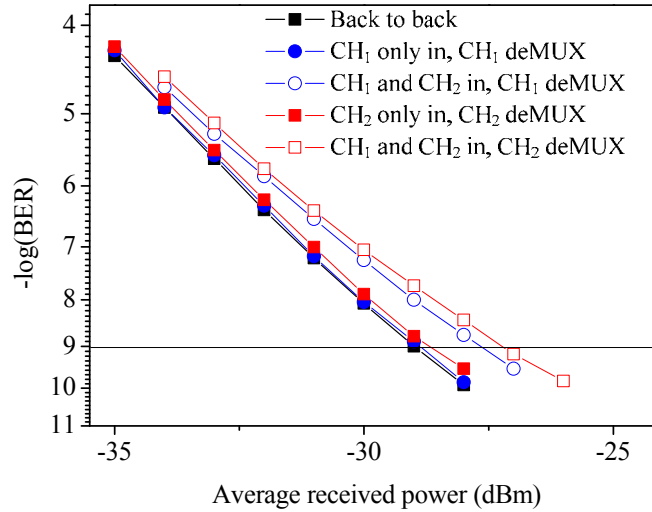


Fig. 8. BER measurements for the two demultiplexed channels with and without crosstalk.

## 5. Conclusion

In conclusion, we have demonstrated an on-chip two-mode multiplexing circuit using a novel  $TE_0$  &  $TE_1$  mode multiplexer built on the SOI platform. The circuit exhibits a lowest insertion loss of 0.3 dB, with mode crosstalk smaller than  $-16$  dB over a wide bandwidth of 100 nm. A large fabrication tolerance of 20 nm and relaxed coupling length sensitivity are experimentally demonstrated. System experiments have been carried out for on-chip two-mode multiplexing application at 40 Gbit/s, showing clear eye diagrams for both demultiplexed channels and 1.6 dB and 1.8 dB power penalties with crosstalk for the two channels, respectively.